Surface Chemistry

Deutsche Ausgabe: DOI: 10.1002/ange.201507104
Internationale Ausgabe: DOI: 10.1002/anie.201507104

Closing the Nanographene Gap: Surface-Assisted Synthesis of Peripentacene from 6,6′-Bipentacene Precursors

Cameron Rogers, Chen Chen, Zahra Pedramrazi, Arash A. Omrani, Hsin-Zon Tsai, Han Sae Jung, Song Lin, Michael F. Crommie, and Felix R. Fischer**

Abstract: *The thermally induced cyclodehydrogenation reaction of 6,6′-bipentacene precursors on Au(111) yields peripentacene stabilized by surface interactions with the underlying metallic substrate. STM and atomic-resolution non-contact AFM imaging reveal rectangular flakes of nanographene featuring parallel pairs of zig-zag and armchair edges resulting from the lateral fusion of two pentacene subunits. The synthesis of a novel molecular precursor 6,6′-bipentacene, itself a synthetic target of interest for optical and electronic applications, is also reported. The scalable synthetic strategy promises to afford access to a structurally diverse class of extended periacenes and related polycyclic aromatic hydrocarbons as advanced materials for electronic, spintronic, optical, and magnetic devices.*

The unusual optical and electronic properties emerging from lateral quantum confinement effects in nanometer-scale flakes of single-layer graphene has inspired the development of novel strategies toward the rational synthesis of atomically defined nanographenes.[1] Among these structures, polycyclic aromatic hydrocarbons (PAHs) featuring uniform edges, that is, acenes or periacenes, are privileged scaffolds.[2] Their pursuit is further motivated by a fundamental interest in the exotic physical properties associated with atomically defined finite boundary conditions in single-layer graphene.[3,4] *n*-Periacenes (**1**; Figure 1) are derived from the lateral fusion of two linear acenes at the *peri*-positions (*n* denotes the number of annulated rings formed through the lateral fusion) into rectangular nanographene flakes. The characteristic structure of *n*-periacene ($n > 1$) exhibits pairs of parallel zig-zag (long-edge) and armchair (short-edge) edges terminated with H-atoms. While the smallest members of this family, perylene ($n = 1$) and bisanthrene ($n = 2$), have been known and studied for decades,[5] the only slightly longer homologues peritetracene ($n = 3$) and peripentacene ($n = 4$) have not been prepared through rational synthesis.[6] Recent resurgent interest in extended *n*-periacenes has been spurred by theoretical calculations predicting an unusual electronic structure, a substantial decrease of the HOMO–LUMO gap upon extending the length of the *n*-periacene, and an antiferromagnetic ground state featuring spin localization along opposing zig-zag edges.[4]

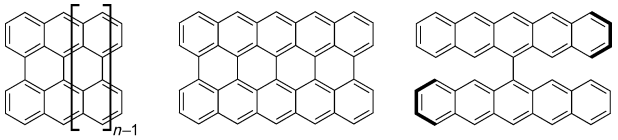

1 2 3

Figure 1. Chemical structure of *n*-periacene (**1**), peripentacene (**2**), and 6,6′-bipentacene (**3**).

Several solution-based synthetic strategies toward laterally extended acenes have been reported, yet the fully cyclized *n*-periacenes ($n > 2$) could not be isolated from these reactions.[6a,7] This has been attributed to the inherent insolubility of unsubstituted acenes, the unusual reactivity of acenes, and their thermal and photochemical instability accredited to a small band gap and significant contributions from resonance structures involving radical character.[2b,3,6a,7a] Experimental signatures for peripentacene (**2**) have thus far only been suggested by mass spectrometry as a potential side product of the thermal decomposition of pentacene, but there has been no structural confirmation for the existence of **2**.[8] Aside from being of fundamental theoretical interest, the extended family of *n*-periacenes have been invoked as promising materials for applications in spintronic, electronic, optical, and magnetic devices.[2b,3,4c,h] Herein we describe the modular, scalable syntheses of bipentacene **3** and its thermally induced cyclodehydrogenation on Au(111) in ultrahigh-vacuum (UHV) to yield surface stabilized, rectangular flakes of peripentacene (**2**). Scanning tunneling microscopy (STM) of both the precursor **3** and the resulting peripentacene itself reveal the superb selectivity and almost quantitative yield of the thermal cyclization process. Atomic-resolution imaging of the cyclodehydrogenation product using non-

[*] C. Rogers,[+] Dr. S. Lin, Prof. Dr. F. R. Fischer
Department of Chemistry, University of California Berkeley
699 Tan Hall, Berkeley, CA 94720 (USA)
E-mail: ffischer@berkeley.edu
C. Chen,[+] Z. Pedramrazi,[+] Dr. A. A. Omrani, H.-Z. Tsai, H. S. Jung, Prof. Dr. M. F. Crommie
Department of Physics, University of California Berkeley
345 Birge Hall, Berkeley, CA 94720 (USA)
E-mail: crommie@berkeley.edu
Dr. S. Lin
Chemical Science Division, Lawrence Berkeley National Laboratory
Berkeley, CA 94720 (USA)
Prof. Dr. M. F. Crommie, Prof. Dr. F. R. Fischer
Materials Science Division, Lawrence Berkeley National Laboratory
Berkeley, CA 94720 (USA)
Prof. Dr. M. F. Crommie, Prof. Dr. F. R. Fischer
Kavli Energy NanoSciences Institute at the University of California Berkeley and the Lawrence Berkeley National Laboratory
Berkeley, CA 94720 (USA)
[+] These authors contributed equally to this work.

Supporting information for this article is available on the WWW under http://dx.doi.org/10.1002/anie.201507104.

contact atomic force microscopy (ncAFM) reveals the detailed structure of peripentacene (**2**).

While syntheses of 6,6′-bipentacene derivatives featuring bulky substituents have been reported, approaches toward the unfunctionalized core **3** have been impeded by poor solubility and the use of thermal transformations at elevated temperatures that are incompatible with the stability of the product.[9] We synthesized the unsubstituted bipentacene **3** through a Staudinger-type diazo-thioketone coupling (Scheme 1). Treatment of pentacen-6(13H)-one (**4**) with

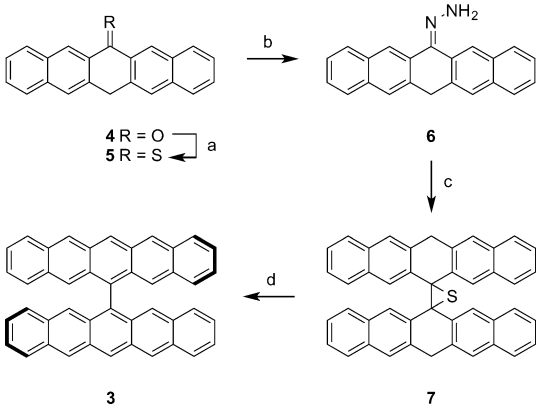

Scheme 1. Synthesis of **3**. Reaction conditions: a) Lawesson's reagent, toluene, 80 °C, 2 h, 62%; b) 1-propanol, hydrazine monohydrate, 120 °C, 3 h, 68%; c) $MgSO_4$, MnO_2, NaOH, MeOH/CH_2Cl_2, 24 °C, 1 h; then **5** CH_2Cl_2, 24 °C, 12 h, 63%; d) LDA, THF, 24 °C, 3 h, 55%.

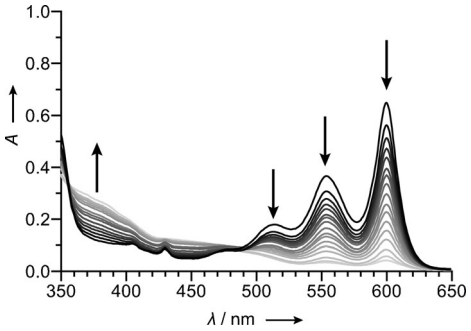

Figure 2. UV/Vis spectra of a dilute solution of bipentacene (**3**) in CH_2Cl_2. Time-dependent UV/Vis spectra of solutions of **3** exposed to air and light were recorded at 15 min intervals (0–4 h).

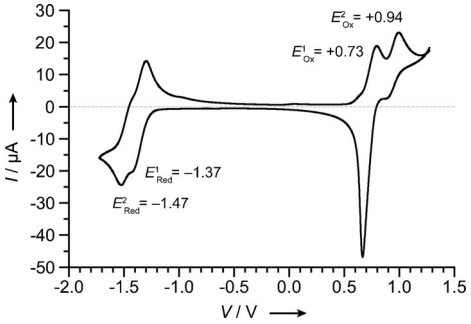

Figure 3. Cyclic voltammogram of **3** in CH_2Cl_2. Oxidation potential E_{Ox} and reduction potential E_{Red}, (reference SCE), are given. Measurement conditions: Bu_4NPF_6 (0.1 M) in CH_2Cl_2; scan rate 100 mV s^{-1}.

hydrazine monohydrate under dehydrating conditions did not yield isolable amounts of hydrazone **6**. If, instead, **4** was converted into the thioketone **5** prior to the reaction with hydrazine, the desired hydrazone **6** was obtained in 60% yield. Oxidation of **6** with MnO_2 gave the corresponding intermediate diazo compound, which was subjected to a 1,3-dipolar cycloaddition with **5** to give the thiirane **7** after loss of N_2. Thiirane **7** contains all 44 C-atoms of bipentacene **3**, including the sterically demanding central C–C bond. Conjugate 1,4-elimination ring-opens the thiirane ring in **7**, followed by H_2S elimination and subsequent rearomatization, to give the bipentacene **3** as a blue powder in 55% yield of isolated product.

UV/Vis spectra of **3** in CH_2Cl_2 (Figure 2) feature a vibrational progression characteristic of extended acenes.[2a] The longest wavelength absorption at $\lambda = 599$ nm ($\varepsilon = 3.7 \times 10^3$ L mol^{-1} cm^{-1}) reveals an optical HOMO–LUMO gap of $\Delta E_{UV/Vis} = 2.07$ eV (pentacene $\Delta E_{UV/Vis} = 2.15$ eV).[10] Dilute solutions of bipentacene **3** exposed to light and air undergo rapid photooxidation. Time-dependent UV/Vis spectra recorded at 15 min intervals indicate a pseudo zero-order reaction with respect to the concentration of **3** and a rate constant $k_{light} = 1.1 \times 10^{-8}$ mol L^{-1} s^{-1} (in the absence of light, the rate of degradation of **3** is $k_{dark} = 1.2 \times 10^{-9}$ mol L^{-1} s^{-1}; Supporting Information, Figure S1). The oxidation of **3** proceeds slower than for the parent pentacene.[11] The steric shielding of the central aromatic ring by the orthogonal arrangement of pentacene subunits obstructs the addition of dioxygen species.[9a,11] Mass spectrometry of photooxidized samples shows the formation of a complex mixture of products resulting from the incorporation of up to seven oxygen atoms (Supporting Information, Figure S2).

We further investigated the electrochemical properties of **3** by cyclic voltammetry (Figure 3) of degassed solutions in CH_2Cl_2 (supporting electrolyte 0.1 M Bu_4NPF_6). Figure 3 shows two reversible one-electron oxidation ($E^1_{Ox} = +0.73$, $E^2_{Ox} = +0.94$ eV) and reduction waves ($E^1_{Red} = -1.37$, $E^2_{Red} = -1.47$ eV) associated with the sequential oxidation/reduction of both pentacene subunits (reference SCE; Supporting Information, Figure S3). The resulting electrochemical HOMO–LUMO gap $\Delta E_{EC} = 2.10$ eV is in good agreement with the optical gap (2.07 eV) derived from UV/Vis spectroscopy. The linear dependence of the peak current on the square root of the scan rate is consistent with a freely diffusing system with facile electron transfer and limiting mass transport (Supporting Information, Figure S4).[12] Notably, **3** shows excellent stability toward electrochemical cycling with no decrease in the peak current over dozens of oxidation and reduction cycles over a large potential range (−2 to +1.5 V).

The fully cyclized peripentacene (**2**) was obtained by sublimation of the bipentacene precursor **3** at 260 °C in UHV onto a Au(111) surface held at 24 °C. STM imaging at 7 K reveals that as-deposited **3** assembles into islands of highly ordered linear chains on the Au surface (Figure 4 A; Supporting Information, Figure S5). The average apparent height of alternating bright spots along a line of self-assembled

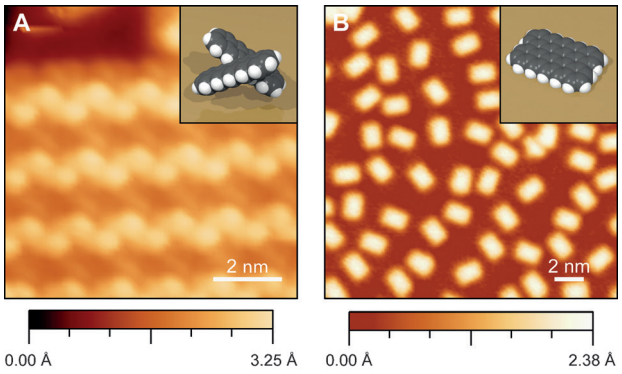

Figure 4. STM images of a Au(111) surface decorated with islands of 6,6′-bipentacene (**3**) and peripentacenes (**2**) following thermally induced cyclodehydrogenation. (A) Constant-current STM image of **3** as deposited on Au(111) ($I = 10$ pA, $V = 0.80$ V, $T = 7$ K). (B) Constant-current STM image of **2** on Au(111) after annealing at 473 K for 30 min ($I = 10$ pA, $V = 0.80$ V, $T = 7$ K). Molecular models are shown in insets.

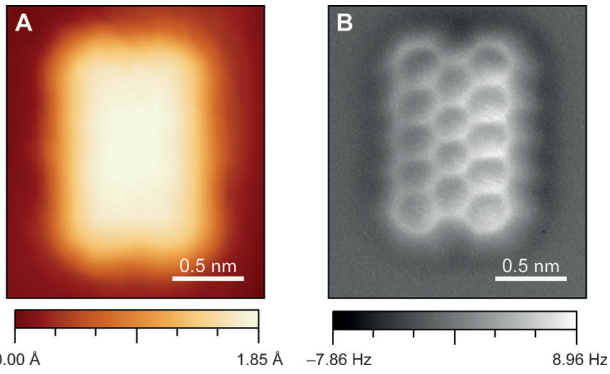

Figure 5. STM and nc-AFM images of a single peripentacene (**2**) on Au(111). (A) Constant-current STM image of **2** ($I = 100$ pA, $V = 0.55$ V, $T = 7$ K). (B) nc-AFM image of **2** (qPlus resonance frequency = 28.73 kHz, Q-value = 8×10^4, oscillation amplitude = 50 pm).

molecules is 2.6 ± 0.1 Å (Supporting Information, Figure S5) with respect to the gold substrate. We associate this periodicity with the preferred dihedral angle adopted between two pentacene subunits in **3** when adsorbed onto the surface (see inset in Figure 4A).

Annealing samples of **3** on Au(111) at 200 °C for 30 min induces a thermal cyclodehydrogenation of all *peri*-positions to form the fully cyclized peripentacene (**2**). STM images (7 K) of **2** reveal a sub-monolayer coverage of the surface with uniform discrete rectangular structures (Figure 4B). The apparent length, width, and height, 1.75 ± 0.04 nm, 1.25 ± 0.04 nm, and 0.21 ± 0.01 nm respectively, match the expected molecular dimensions of peripentacene **2** (Supporting Information, Figures S6, S7). Figure 4B shows a typical STM image illustrating the high yield and remarkable selectivity of the thermally induced cyclodehydrogenation reaction. Fewer than 5% of the adsorbed molecules deviate from the expected rectangular shape (a large area image is shown in the Supporting Information, Figure S8). Scanning tunneling spectroscopy (STS) performed on fully cyclized peripentacene **2** on Au(111) does not reveal distinctive features within a bias range from −0.6 V to 0.5 V (Supporting Information, Figure S9).

To unequivocally assign the structure of the cyclization product **2** we performed subnanometer-resolved ncAFM imaging using a low-temperature qPlus-equipped commercial Omicron LT-STM/AFM at $T = 4.5$ K (Figure 5B).[13,14] The apex of the gold-coated tungsten STM tip was functionalized with a single CO molecule prior to imaging. Contrast in nc-AFM images arises from the frequency shift of the qPlus resonator while scanning over the molecule in constant height mode. Samples of molecule-decorated Au(111) surfaces were prepared following the deposition/annealing sequence outlined above. Unlike the diffuse STM topographic image (Figure 5A), which reflects frontier orbital local density of states, the ncAFM image (Figure 5B) reveals not only the exact position of carbon atoms but also the intramolecular bonds forming the aromatic carbon skeleton of **2**. Figure 5B clearly shows the two parallel-aligned zig-zag edges of **2** that are predicted to lead to exotic electronic/magnetic behavior in extended periacenes. The interaction of peripentacene with the free valences of the Au(111) surface stabilize this highly reactive molecule and prevent undesired radical side reactions that have thus far prevented the isolation of **2** from solution-based reactions.

In summary, we report the first successful preparation of peripentacene (**2**) and its detailed characterization by STM and subnanometer-resolved ncAFM. The synthetic strategy makes use of a Staudinger-type diazo-thioketone coupling, followed by a late-stage aromatization to give the metastable intermediate 6,6-bipentacene. Surface-assisted cyclodehydrogenation produces the peripentacene in excellent yields and high selectivity. This synthetic method has the potential to provide access to the experimental investigation of extended acenes predicted to exhibit exotic ground-state electronic configurations. Periacenes and related materials, long the subject of only theoretical investigation, are now more accessible for practical study and application.

Acknowledgements

Research supported by the U.S. Department of Energy (DOE), Office of Science, Basic Energy Sciences (BES), under award no. DE-SC0010409 (design, synthesis and characterization of molecules) and Nanomachine Program award no. DE-AC02-05CH11231 (surface reaction characterization), by the Office of Naval Research BRC Program (peripentacene ncAFM imaging), and by the National Science Foundation award no. DMR-1206512 (image analysis); Berkeley NMR Facility is supported in part by NIH grant SRR023679A. A.A.O. acknowledges support from Swiss National Science Foundation (SNSF) Postdoctoral Research Fellowship under Grant No. P2ELP2-151852.

Keywords: arenes · graphene · non-contact AFM · periacene · surface chemistry

How to cite: *Angew. Chem. Int. Ed.* **2015**, *54*, 15143 – 15146
Angew. Chem. **2015**, *127*, 15358 – 15361

[1] A. Narita, X.-Y. Wang, X. Feng, K. Müllen, *Chem. Soc. Rev.* **2015**, *44*, 6616 – 6643.
[2] a) J. Anthony, *Angew. Chem. Int. Ed.* **2008**, *47*, 452 – 483; *Angew. Chem.* **2008**, *120*, 460 – 492; b) Q. Ye, C. Chi, *Chem. Mater.* **2014**, *26*, 4046 – 4056.
[3] a) Z. Sun, Q. Ye, C. Chi, J. Wu, *Chem. Soc. Rev.* **2012**, *41*, 7857 – 7889; b) Z. Sun, Z. Zeng, J. Wu, *Chem. Asian J.* **2013**, *8*, 2894 – 2904.
[4] a) D. Jiang, B. Sumpter, S. Dai, *J. Chem. Phys.* **2007**, *127*, 124703; b) D. Jiang, S. Dai, *Chem. Phys. Lett.* **2008**, *466*, 72 – 75; c) H. Şahin, R. Senger, *Phys. Rev. B* **2008**, *78*, 205423; d) F. Moscardó, E. San-Fabián, *Chem. Phys. Lett.* **2009**, *480*, 26 – 30; e) B. Pham, T. Truong, *Chem. Phys. Lett.* **2012**, *535*, 75 – 79; f) P. Rivero, C. Jiménez-Hoyos, G. Scuseria, *J. Phys. Chem. B* **2013**, *117*, 12750 – 12758; g) F. Plasser, H. PaŠalić, M. Gerzabek, F. Libisch, R. Reiter, J. Burgdörfer, T. Müller, R. Shepard, H. Lischka, *Angew. Chem. Int. Ed.* **2013**, *52*, 2581 – 2584; *Angew. Chem.* **2013**, *125*, 2641 – 2644; h) S. Muhammad, H. Xu, R. Zhong, Z. Su, A. Al-Sehemi, A. Irfan, *J. Mater. Chem. C* **2013**, *1*, 5439 – 5449.
[5] a) E. Clar, *Chem. Ber.* **1948**, *81*, 52 – 63; b) E. Fort, P. Donovan, L. Scott, *J. Am. Chem. Soc.* **2009**, *131*, 16006 – 16007; c) J. Li, K. Zhang, X. Zhang, K. Huang, C. Chi, J. Wu, *J. Org. Chem.* **2009**, *74*, 856 – 863; d) E. Fort, L. Scott, *Angew. Chem. Int. Ed.* **2010**, *49*, 6626 – 6628; *Angew. Chem.* **2010**, *122*, 6776 – 6778; e) A. Konishi, Y. Hirao, M. Nakano, A. Shimizu, E. Botek, B. Champagne, D. Shiomi, K. Sato, T. Takui, K. Matsumoto, H. Kurata, T. Kubo, *J. Am. Chem. Soc.* **2010**, *132*, 11021 – 11023; f) Y. Hirao, A. Konishi, K. Matsumoto, H. Kurata, T. Kubo, *AIP Conf. Proc.* **2012**, *1504*, 863 – 866.
[6] a) L. Zöphel, R. Berger, P. Gao, V. Enkelmann, M. Baumgarten, M. Wagner, K. Müllen, *Chem. Eur. J.* **2013**, *19*, 17821 – 17826; b) R. Dorel, C. Manzano, M. Grisolia, W. Soe, C. Joachim, A. Echavarren, *Chem. Commun.* **2015**, *51*, 6932 – 6935; c) A. Matsumoto, M. Suzuki, D. Kuzuhara, H. Hayashi, N. Aratani, H. Yamada, *Angew. Chem. Int. Ed.* **2015**, *54*, 8175 – 8178; *Angew. Chem.* **2015**, *127*, 8293 – 8296; d) J. Liu, P. Ravat, M. Wagner, M. Baumgarten, X. Feng, K. Müllen, *Angew. Chem. Int. Ed.* **2015**, *54*, 12442 – 12446; *Angew. Chem.* **2015**, *127*, 12619 – 12623.
[7] a) X. Zhang, J. Li, H. Qu, C. Chi, J. Wu, *Org. Lett.* **2010**, *12*, 3946 – 3949; b) A. Konishi, Y. Hirao, K. Matsumoto, H. Kurata, T. Kubo, *Chem. Lett.* **2013**, *42*, 592 – 594; c) A. Konishi, Y. Hirao, K. Matsumoto, H. Kurata, R. Kishi, Y. Shigeta, M. Nakano, K. Tokunaga, K. Kamada, T. Kubo, *J. Am. Chem. Soc.* **2013**, *135*, 1430 – 1437.
[8] L. Roberson, J. Kowalik, L. Tolbert, C. Kloc, R. Zeis, X. Chi, R. Fleming, C. Wilkins, *J. Am. Chem. Soc.* **2005**, *127*, 3069 – 3075.
[9] a) X. Zhang, X. Jiang, J. Luo, C. Chi, H. Chen, J. Wu, *Chem. Eur. J.* **2010**, *16*, 464 – 468; b) S. Li, Z. Jia, K. Nakajima, K. Kanno, T. Takahashi, *J. Org. Chem.* **2011**, *76*, 9983 – 9987; c) K. Tanaka, N. Aratani, D. Kuzuhara, S. Sakamoto, T. Okujima, N. Ono, H. Yamada, *RSC Adv.* **2013**, *3*, 15310 – 15315.
[10] J. B. Birks, *Photophysics of Aromatic Molecules*, Wiley-Interscience, New York, **1970**.
[11] I. Kaur, W. Jia, R. Korpreski, S. Selvarash, M. Dokmeci, C. Pramanik, N. McGruer, G. Miller, *J. Am. Chem. Soc.* **2008**, *130*, 16274 – 16286.
[12] A. J. Bard, L. R. Faulkner, *Elelctrochemical Methods: Fundamentals and Applications*, Wiley, Hoboken, **2000**.
[13] a) L. Gross, F. Mohn, N. Moll, P. Liljeroth, G. Meyer, *Science* **2009**, *325*, 1110 – 1114; b) L. Gross, F. Mohn, N. Moll, P. Liljeroth, G. Meyer, R. Ebel, W. M. Abdel-Mageed, M. Jaspares, *Nat. Chem.* **2010**, *2*, 821 – 825.
[14] a) F. J. Giessibl, *Appl. Phys. Lett.* **1998**, *73*, 3956 – 3958; b) F. J. Giessibl, *Appl. Phys. Lett.* **2000**, *76*, 1470 – 1472; c) F. J. Giessibl, *Rev. Mod. Phys.* **2003**, *75*, 949 – 983.

Received: July 30, 2015
Revised: September 8, 2015
Published online: October 20, 2015

